JOURNAL OF COMPUTATIONAL BIOLOGY
Volume 23, Number 0, 2016

Pp. 1–14
DOI: 10.1089/cmb.2016.0059

Research Article

Bioinformatics Prediction and Experimental Validation of MicroRNAs Involved in Cross-Kingdom Interaction

STEFANO PIRRÒ,[1,2] ANTONELLA MINUTOLO,[1] ANDREA GALGANI,[1,2] MARINA POTESTÀ,[1] VITTORIO COLIZZI,[1,2] and CARLA MONTESANO[1]

ABSTRACT

MicroRNAs (miRNAs) are a class of small noncoding RNAs that act as efficient post-transcriptional regulators of gene expression. In 2012, the first cross-kingdom miRNA-based interaction had been evidenced, demonstrating that exogenous miRNAs act in a manner of mammalian functional miRNAs. Starting from this evidence, we defined the concept of cross-kingdom functional homology between plant and mammalian miRNAs as a needful requirement for vegetal miRNA to explicit a regulation mechanism into the host mammalian cell, comparable to the endogenous one. Then, we proposed a new dedicated algorithm to compare plant and mammalian miRNAs, searching for functional sequence homologies between them, and we developed a web software called MirCompare. We also predicted human genes regulated by the selected plant miRNAs, and we determined the role of exogenous miRNAs in the perturbation of intracellular interaction networks. Finally, as already performed by Pirrò and coworkers, the ability of MirCompare to select plant miRNAs with functional homologies with mammalian ones has been experimentally confirmed by evaluating the ability of *mol-miR168a* to downregulate the protein expression of SIRT1, when its mimic is transfected into human hepatoma cell line G2 (HEPG2) cells. This tool is implemented into a user-friendly web interface, and the access is free to public through the website http://160.80.35.140/MirCompare

Key words: computational molecular biology, microRNA, sequence analysis.

1. INTRODUCTION

MicroRNAs (miRNAs) are a class of small (17–25 nucleotides) noncoding RNAs that post-transcriptionally regulate gene expression by interacting with mRNAs. In the past, miRNAs have been strongly associated with the regulation of critical biological events, including development, differentiation, inflammation, apoptosis, and carcinogenesis (Frixa et al., 2015; Sadovsky et al., 2015; Cui et al., 2016; Dileepan et al., 2016; Gurtner et al., 2016; Lee et al., 2016; Li and Sarkar, 2016; Li et al., 2016; Xie et al., 2016).

The miRNA-mediated gene regulation may occur either through mRNA degradation or preventing mRNA from being translated. Plant miRNAs need high complementarity to recognize their substrate, and the target cleavage is considered the predominant pathway to repress gene expression. Several studies

[1]Department of Biology, University of Rome ''Tor Vergata,'' Rome, Italy.
[2]Mir-Nat s.r.l., Rome, Italy.

suggest that translational inhibition is also a common mechanism used by plant miRNAs to repress gene expression. In animals, the semicomplementary interaction leads to silencing achieved by translational repression (Mallory et al., 2004; Bartel, 2009; Huang et al., 2010; Liu et al., 2014; Xie et al., 2015). In 2013, Brennecke et al. (2005) described for the first time the minimal requirements for a functional miRNA:mRNA-target duplex in vivo. The study reported that any mismatch in positions 2–8 of the seed region strongly reduced the magnitude of the target regulation. Moreover, the minimal 5′ sequence complementarity necessary to confer target regulation is of four or five nucleotides. Although many studies have reported the cross-kingdom transfer between animals and parasites, plants and viruses (LaMonte et al., 2012; Feng and Chen, 2013; Buck et al., 2014; Han and Luan, 2015), in 2012, Zhang et al. demonstrated for the first time that *osa-miR168a* and other exogenous miRNAs abundant in rice plants are present in the sera and tissues of mice acquired orally through food intake. Functional studies in vitro and in vivo demonstrated that *osa-miR168a* binds the human/mouse low-density lipoprotein receptor adapter protein 1 (*LDLRAP1*) mRNA, inhibits the expression of protein in liver, and decreases the LDL removal from mouse plasma (Zhang et al., 2011). For the first time, Zhang and collaborators demonstrated that miRNAs contained in vegetal food regulate mRNA translation in a manner of mammalian functional miRNAs.

Although there are controversial opinions about the presence of small RNAs in tissues and the efficiency of dietary ingestion as the mechanism of cross-kingdom delivery (Dickinson et al., 2013; Snow et al., 2013), recently, it has been demonstrated that abundance in the serum of plant *miR159* was inversely correlated with breast cancer incidence and progression in patients (Chin et al., 2016). As stated by the authors, these results demonstrate for the first time that a plant miRNA can inhibit cancer growth in mammals. Moreover, miRNA profiles of several plants with alimentary and medical interest have been sequenced to better investigate the sensible regulation process behind these molecules (Baldrich and San Segundo, 2016; Pirrò et al., 2016).

During the past years, several computational approaches such as miRanda (John et al., 2004), TargetScan (Lewis et al., 2005), PITA (Kertesz et al., 2007), and PicTar (Krek et al., 2005) have been elaborated to predict miRNA:mRNA interactions.

Most algorithms use experimental knowledge to develop a specific scoring system such as miRNA:mRNA partial complementarity, seed region, target position, and sequence conservation features. In 2013, Coronnello and Benos developed a web tool for combinatorial miRNA target prediction called COMIR, which combines four popular scoring schemes (miRanda, PITA, TargetScan, and mirSVR) to compute the potential of a gene to be targeted by a set of miRNAs (Coronnello and Benos, 2013).

In 2015, Shu presented comparative analysis and computational predictions of miRNAs that can be transferred into human circulation (Shu et al., 2015). However, no bioinformatic studies have been carried out to design, implement, and validate an algorithm to predict the action of plant miRNAs inside the mammalian host cell environment leading to cross-kingdom interactions.

For this reason, we rationalized the required sequence homologies between plant and mammalian miRNAs, suggesting for the first time the concept of cross-kingdom functional homology, and we developed MirCompare, a web application based on a strategy for the comparison between plant and mammalian miRNAs and their highly stringent selection to identify some possible plant miRNAs, with functional homologies with mammalian ones. Moreover, we conducted preliminary analysis to investigate potential human gene regulation by *miR168a* mimic from *Moringa oleifera* Lam. The reported analysis increases the information on plant miRNAs currently available and improves the knowledge on to the molecular mechanisms associated with nutritional and medicinal activities of this plant species.

2. MIRCOMPARE DEVELOPMENT

According to Zhang et al. (2011), plant miRNAs in mammalian cells use the endogenous machinery to post-transcriptionally regulate their target genes.

Starting from this fundamental evidence, we propose a model where plant and mammalian miRNAs share the same gene targets if they show the following: (1) a sequence homology rate higher than a specific percentage and (2) a strict sequence homology related to the seed region.

MirCompare is based on an algorithm able to compare libraries of miRNAs belonging to organisms from plant and animal kingdoms, to find cross-kingdom functional homologies. As shown in Figure 1, the computational process is divided in two main phases—comparison and filtering.

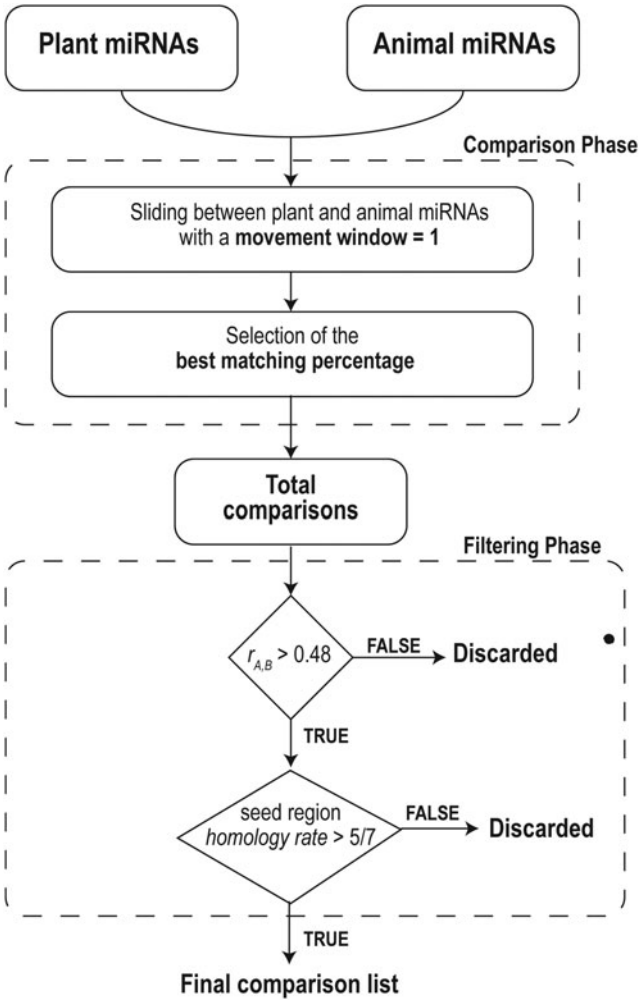

FIG. 1. Workflow of the MirCompare algorithm. In the comparison phase, we evaluate the best alignment rate between each couple of miRNAs. In the filtering phase, we select only functional homologies using a double-step approach based on the evaluation of the overall homology and the seed region stringency.

2.1. Comparison phase

To evaluate the best alignment rate between each couple of miRNAs (A and B), the shorter sequence is sliding on the longer one, using a sliding window of 1 nucleotide, and for each step, an alignment score $S_{A,B}$ is calculated.

$$S_{A,B} = \frac{matches_{A,B}}{\max(length(A), length(B))} \tag{1}$$

When all the possible alignment rates for each couple of uploaded miRNAs have been generated, the algorithm selects the best comparison rate (r):

$$r_{A,B} = \max_i(S_{A,B}) \tag{2}$$
$$\text{where } 0 \leq i \leq \max(length(A), length(B)) - 1$$

The comparison phase computes a total of $N \times M$ different comparison rates, where N and M are, respectively, the length of the first and second miRNA data sets.

2.2. Filtering phase

In the filtering phase, the rules for the cross-kingdom functional sequence homology are applied. The process can be subdivided into two parts as follows. (1) Filter based on the overall sequence homology rate and (2) selection related to the seed region sequence homology.

To identify a cutoff for the best comparison rate between each miRNA couple ($r_{A,B}$), 10^4 and 10^6 stochastic comparisons were generated, using two scramble sets of 10^2 and 10^3 sequences, respectively (Fig. 2A, B). According to Wang et al. (Wang, 2013), base composition of mammalian miRNAs show an evolutionary conservation and are GU rich. For this reason, we decided to build the sets of random sequences according to the experimental evidences. More in detail, each set is composed of sequences of length between 17 and 25 nucleotides with a percentage of A and C of 20% and G and U of 30%. To establish the minimum *r*-value threshold able to produce a statistically significant alignment between a couple of miRNA sequences (if the comparison between a couple of miRNAs is better than we would expect between any two random sequences), we plotted the *r*-value frequency distribution in above described stochastic comparison analysis (Fig. 2A, B).

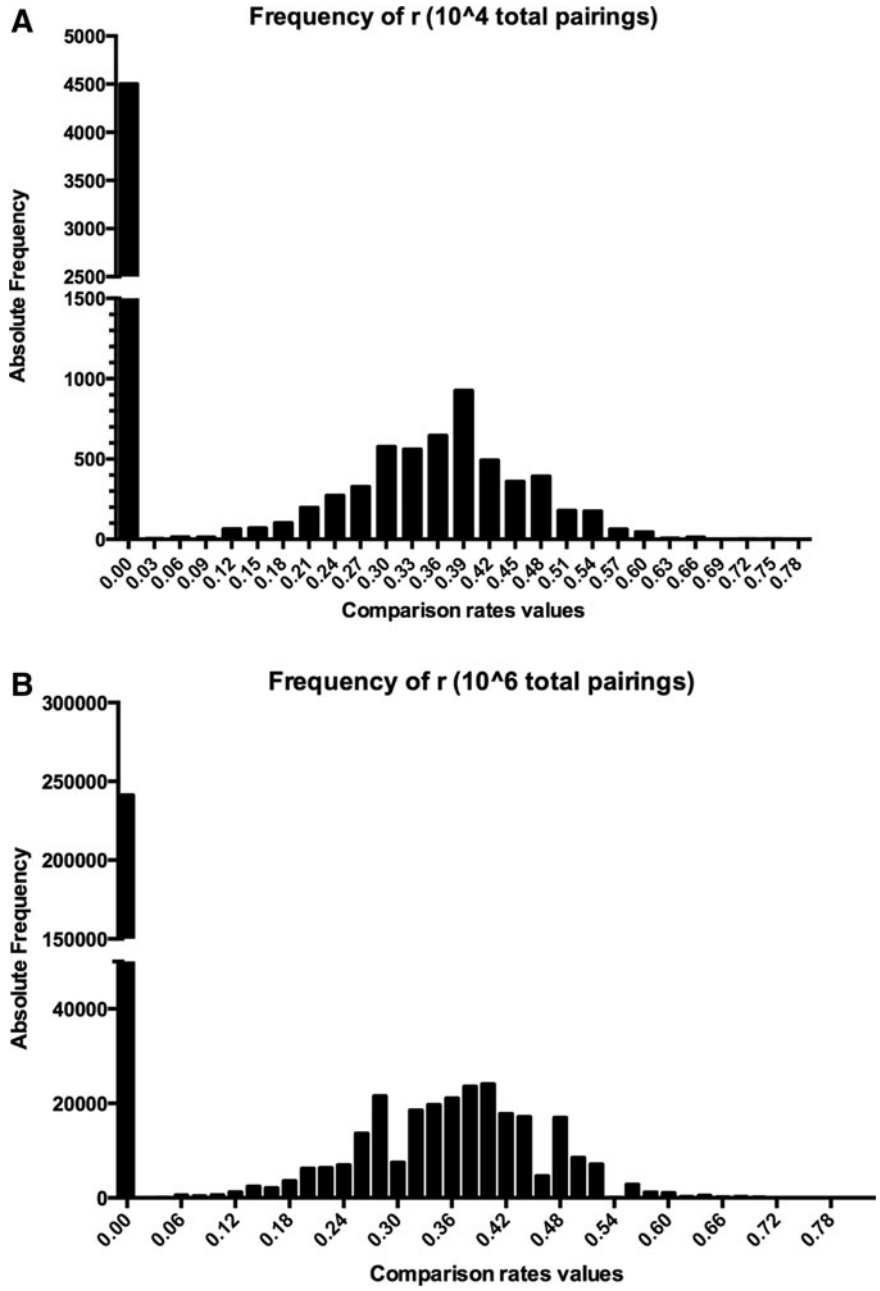

FIG. 2. *r*-Value frequency distribution in two stochastic analysis involving 10^4 **(A)** and 10^6 **(B)** comparisons.

For each generated *r*-value, we calculated a *p*-value defined as follows:

$$pvalue = \frac{\sum(num.occurrences(r_{A,B}) | r_{A,B} \geq threshold)}{\sum(num.occurrences(r_{A,B}))} \quad (3)$$

In both the casual comparisons, a peak on 0 has been observed, confirming the casualty of the alignment. Looking at the *r*-value distributions, we also obtained similar statistically significant cutoffs. In the case of 10^4 comparisons, the lowest threshold value that generates a *p*-value ≤0.05, is 0.48, while in the case of 10^6, it is 0.46. For this reason, we decided to fix the *r*-value threshold at 0.48. MirCompare gives the possibility to arbitrarily change this value according to the desired stringency of the analysis.

Functional studies from Brennecke et al. (2005) have been conducted to identify the minimal requirements for a functional miRNA–target duplex in vivo. The magnitude of target regulation is not affected by a mismatch at positions 1, 9, or 10, but any mismatch from positions 2 to 8 causes a strong reduction. In addition, a minimal complementarity of four or five nucleotides into the seed region is necessary to confer target regulation. Therefore, we applied an additional filter, selecting only the comparisons that show a homology rate value higher than five out of seven nucleotides, into the seed region.

2.3. Computational analysis

2.3.1. Prediction of miRNA targets. To predict all the possible cross-kingdom targets in humans, we assumed that plant miRNAs regulate host mRNA translation in an analogous manner of mammalian functional miRNAs. To this end, the COMIR web tool (Coronnello and Benos, 2013) was used to rank human genes by their propensity to be regulated by human miRNAs showing functional homology with the plant ones. The COMIR output is provided as a list of ''target gene–miRNA–COMIR score'' elements.

2.3.2. Protein interaction analysis. The mentha interactome browser (Calderone et al., 2013) has been used to retrieve protein interaction network of the top predicted plant-regulated human genes and their first neighbor. Cytoscape software (Shannon et al., 2003) was used to manage the extracted network to filter relationships on the propensity of a couple of proteins to interact. The lowest threshold was set to 0.7.

2.3.3. Analysis on sequence conservation. To evaluate the conservation of *miR168a* in all sequenced plant species, Clustal 2.1 (Larkin et al., 2007) has been used.

2.4. Experimental validation of miRNA-mRNA cross-kingdom interaction

2.4.1. Transfection. We studied the biological activity of the synthetic *mol-miR168a* (UCGCUU GGUGCAGGUCGGGAC) that was transfected into the hepatocellular carcinoma cell line (HEPG2) by the Lipofectamine method (Hi-Fect; Qiagen) in accordance with the manufacturer's instruction (miRNA mimic and inhibitor experiment protocols; Qiagen) as already described (Pirrò et al., 2016).

2.4.2. Western blot analysis. Western blot analysis was performed in triplicate biological replication using the experimental procedure already described (Pirrò et al., 2016).

3. RESULTS

3.1. Selection of M. oleifera miRNAs

In 2016, Pirrò and collaborators analyzed miRNA populations obtained from seeds of *M. oleifera* (Pirrò et al., 2016), with the aim of investigating a possible miRNA-mediated regulation process behind its medicinal factor. MirCompare has been used to identify *M. oleifera* miRNAs with functional homologies with human ones, comparing *M. oleifera* and *Homo sapiens* miRNomes.

As shown in Figure 3, the analysis of 98 *M. oleifera* (94 conserved and 4 novel) and 2042 *H. sapiens* miRNAs (www.mirbase.org) (Kozomara and Griffiths-Jones, 2010) generated a total of 285,880 different comparisons.

The exclusion of those with an *r*-value lower than 0.55, allowed to reduce the number to 904. After the second filtering phase over the seed region, only nine different comparisons have been obtained (Table 1) that involved eight *M. oleifera* and nine *H. sapiens* different miRNAs. As reported also in Pirrò et al. (2016), the *mol-miR166i* resulted in functional homologies with *hsa-miR6503-3p* that is involved in regulating inflammation (Ma et al., 2015), and *mol-miR393c* was homologous to *hsa-miR548ah-5p* that is involved in immune tolerance (Xing et al., 2015). Furthermore, *mol-miR168a* showed sequence homology with *hsa-miR579*, a human miRNA that normally regulates TNFα expression during endotoxin tolerance (El Gazzar and McCall, 2010).

3.2. *Computational prediction of human genes regulated by* M. oleifera *miRNAs*

The COMIR web tool (Coronnello and Benos, 2013) was used to compute the potential of a human gene to be targeted by each *M. oleifera* miRNA highlighted by MirCompare (Table S2, Pirrò et al., 2016).

To better understand the putative role of exogenous miRNAs in the alteration of intracellular interaction networks, we selected the top 10 human genes for each *M. oleifera* miRNA (Table S2, Pirrò et al., 2016), and we built a protein interaction network (PPI) using the mentha interactome browser (Calderone et al.,

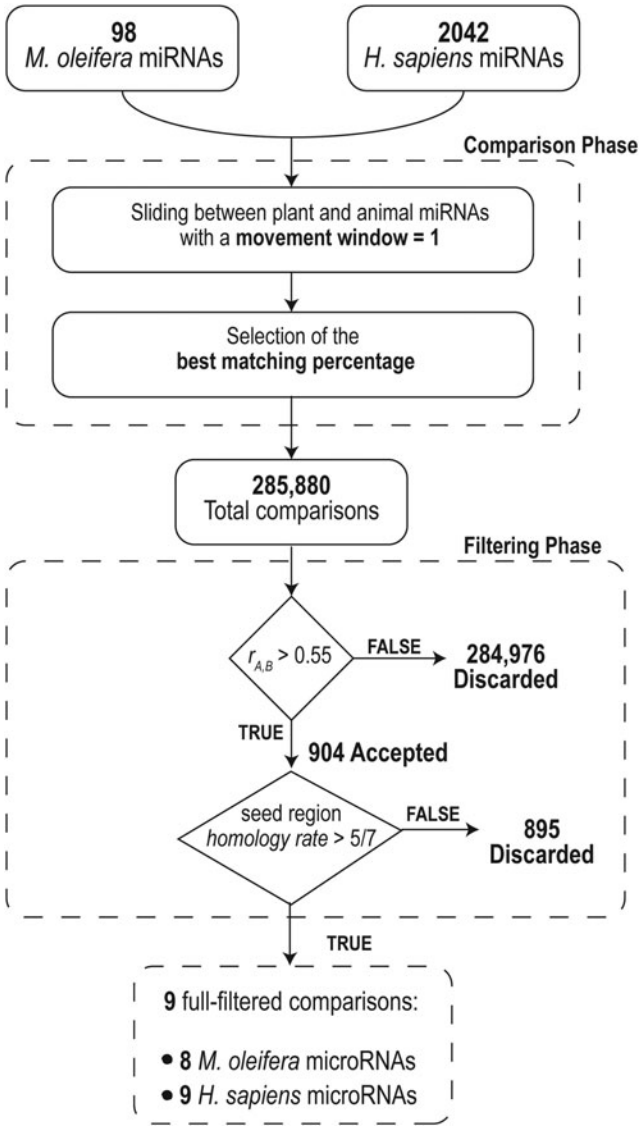

FIG. 3. Schematization of MirCompare analysis between *M. oleifera* and *H. sapiens* microRNAs.

Table 1. MirCompare Results for the Comparison Between *Moringa oleifera* MicroRNAs and Their Human Homologs (Pirrò et al., 2016)

Homo sapiens *miRNA*	Moringa oleifera *miRNA*	r-*Value*	*Seed mismatch*	*Alignment detail*
hsa-miR6503-3p	*mol-miR166i*	0.67	2	-GGAC-AGG-U-CA--CC-CC
hsa-miR548ah-5p	*mol-miR393c*	0.65	2	-AAAG-GAU-GCA-UG-U--
hsa-miR3940-5p	*mol-miR159a*	0.65	2	-UGG-UUG--G-G-GCUCU-
hsa-miR579	*mol-miR168a*	0.57	2	UC--UUGGU--A---CG-GA-
hsa-miR4534	*mol-miR159a*	0.71	1	GGAU-GA-G-G-G-UCU
hsa-miR1306-3p	*mol-miR6478*	0.78	1	AC-UU-GCUC-G-UGGUG
hsa-miR4703-3p	*mol-miR6300*	0.72	1	GU-GUUGUA-U-UA-UG-
hsa-miR5008-5p	*mol-miR6300*	0.67	2	G-C-UUG--G-A-AGUGG
hsa-miR4273	*mol-miR398c*	0.67	0	GUGUUCUC-G-U-G-C--

miRNAs, microRNAs.

2013). Mentha classifies interaction on type and method to assign a reliability score to each binary (protein A, protein B) interaction. The reliability score was used to filter the PPI network from the intrinsic noise of PPI information due to contradictory PPI information, inconsistent data curation, or curation errors. We set up a minimum score of 0.7 to filter interactions.

As described in Table 2, *mol-miR168a* regulates the expression of SIRT1, a hub protein with a key role in regulating cellular pathways such as apoptosis, cell cycle, and protein degradation. As shown in Figure 4 SIRT1 is a highly reliable direct interactor of P53 (Langley et al., 2002; Kim et al., 2007, 2008; Zhao et al., 2008; Inoue et al., 2011; Liu et al., 2011; Jain et al., 2012; Gonfloni et al., 2014). Moreover, SIRT1 is significantly elevated in human prostate cancer (Huffman et al., 2007), acute myeloid leukemia (Bradbury et al., 2005), and primary colon cancer (Stünkel et al., 2007). Based on these experimental evidences, we decided to focus our attention on *mol-miR168a* for further analysis.

3.3. *Conservation analysis of plant* miR168a *family*

As well described by Zhang and coworkers (Jones-Rhoades, 2011), an analysis on 481 miRNAs in 71 different plant species showed that *miR168* family is found in at least 10 plant families and can be considered as highly conserved miRNA. In addition, high levels of *bdi-miR168* and *zma-miR168a* have been identified inside human and porcine breast milk exosomes, respectively (Lukasik and Zielenkiewicz, 2014). To understand how small variations in the miRNA sequence could affect the action in human cells, we first evaluated the conservation rate of *mol-miR168a* in 18 plant organisms stored inside miRBase (Kozomara and Griffiths-Jones, 2010). Sequence alignment details (Fig. 5A) and the related dendrogram (Fig. 5B) show the presence of three distinct clusters of sequences (Fig. 5C), which differ in one to two bases. The *miR168a* from *Olea europaea* showed discordance in 3′ and 5′ ends that may be related to a bias in the Illumina trimming process (Del Fabbro et al., 2013).

MirCompare was used to determine the relationship between conservation in sequence and functional homology with human miRNAs. As shown in Figure 6A, *Arabidopsis thaliana, Oryza sativa*, and *M. oleifera* groups share a total of 13 human miRNas that includes *hsa-miR579.* To study the dependency between miRNAs sequence conservation and action in human cells, independent COMIR (Coronnello and Benos, 2013) analysis on each plant *miR168a* was conducted. As clearly shown in Figure 6B, the three clusters of sequences share a total of 6244 genes (86.9%), and *SIRT1* is included in this group.

3.4. *Transfection efficiency and protein modulation*

The formal evidence that *mol-miR168a* identified by MirCompare inhibits the translation of SIRT1 when their synthetic mimics are transfected into the cancer cell line HEPG2 was previously demonstrated (Pirrò et al., 2016) and described here in Figure 7. As shown in Figure 7A, the efficiency of transfection has been assessed monitoring the increase of the percentage of fluorescent-positive (FL1-positive) cells by flow cytometry analysis. To confirm the effect of miRNA treatment, we have investigated the protein expression of SIRT1, a specific target of *hsa-miR579* homologous of *mol-miR168a*. The transfection of mimics derived

Table 2. Top 10 Human Gene Targets Predicted with COMIR Software (Pirrò et al., 2016)

M. oleifera *miRNA*	*ENSEMBLE gene ID*	*Entrez ID*	*Gene name*	*COMIR score*
mol-miR166i	ENSG00000082701	2932	*GSK3B*	0.9019
	ENSG00000064393	28996	*HIPK2*	0.9076
	ENSG00000156113	3778	*KCNMA1*	0.9038
	ENSG00000263162	8924 100653292	*HERC2*	0.9074
	ENSG00000169213	5865	*RAB3B*	0.9075
	ENSG00000171105	3643	*INSR*	0.9015
	ENSG00000078142	5289	*PIK3C3*	0.9044
	ENSG00000263162	8924 100653292	*HERC2*	0.9074
	ENSG00000119547	9480	*ONECUT2*	0.9075
mol-miR393c	ENSG00000178662	80034	*CSRNP3*	0.9075
	ENSG00000102908	10725	*NFAT5*	0.9074
	ENSG00000128585	4289	*MKLN1*	0.9074
	ENSG00000145907	10146	*G3BP1*	0.9074
	ENSG00000009413	5980	*REV3L*	0.9072
	ENSG00000010244	7756	*ZNF207*	0.9072
	ENSG00000100354	23112	*TNRC6B*	0.9072
	ENSG00000143190	5451	*pou2f1*	0.9072
	ENSG00000173611	286205	*Scai*	0.9072
	ENSG00000100731	22990	*Pcnx*	0.9071
mol-miR159a	ENSG00000171435	283455	*KSR2*	0.9076
	ENSG00000119547	9480	*ONECUT2*	0.9076
	ENSG00000153721	154043	*CNKSR3*	0.9074
	ENSG00000261115	1.01E+08	*TMEM178B*	0.9074
	ENSG00000158445	3745	*KCNB1*	0.9072
	ENSG00000077157	4660	*PPP1R12B*	0.907
	ENSG00000196090	11122	*PTPRT*	0.907
	ENSG00000055609	58508	*KMT2C*	0.9068
	ENSG00000132549	157680	*VPS13B*	0.9065
	ENSG00000148019	84131	*CEP78*	0.9062
mol-miR168a	ENSG00000096717	23411	*SIRT1*	0.9087
	ENSG00000178562	940	*CD28*	0.9099
	ENSG00000134352	3572	*IL6ST*	0.9237
	ENSG00000118689	2309	*FOXO3*	0.919
	ENSG00000106799	7046	*TGFBR1*	0.9115
	ENSG00000169967	10746	*MAP3K2*	0.9118
	ENSG00000175595	2072	*ERCC4*	0.911
	ENSG00000149311	472	*ATM*	0.9187
	ENSG00000149948	8091	*HMGA2*	0.9119
	ENSG00000007372	5080	*PAX6*	0.9189
mol-miR6478	ENSG00000134313	57498	*KIDINS220*	0.9061
	ENSG00000106261	7586	*ZKSCAN1*	0.9058
	ENSG00000134909	9743	*ARHGAP32*	0.9055
	ENSG00000136709	55339 84826	*WDR33*	0.9055
	ENSG00000112706	3617	*IMPG1*	0.9051
	ENSG00000107331	20	*ABCA2*	0.9049
	ENSG00000088808	23368	*PPP1R13B*	0.9029
	ENSG00000167654	85300	*ATCAY*	0.9028
	ENSG00000189339	728661	*SLC35E2B*	0.9026
	ENSG00000180370	5062	*PAK2*	0.9025
mol-miR6300	ENSG00000178567	9852	*EPM2AIP1*	0.9076
	ENSG00000213699	54978	*SLC35F6*	0.9075
	ENSG00000197818	23315	*SLC9A8*	0.9072
	ENSG00000183751	10607	*TBL3*	0.9071
	ENSG00000206190	57194	*ATP10A*	0.9071
	ENSG00000166206	2562	*GABRB3*	0.9071

(*continued*)

TABLE 2. (CONTINUED)

M. oleifera *miRNA*	*ENSEMBLE gene ID*	*Entrez ID*	*Gene name*	*COMIR score*
	ENSG00000198000	55035	*NOL8*	0.907
	ENSG00000172380	55970	*GNG12*	0.907
	ENSG00000152443	284309	*ZNF776*	0.9067
	ENSG00000133703	3845	*KRAS*	0.9066
mol-miR398c	ENSG00000055609	58508	*KMT2C*	0.9076
	ENSG00000164684	619279	*ZNF704*	0.9076
	ENSG00000145012	4026	*LPP*	0.9076
	ENSG00000151914	667	*DST*	0.9075
	ENSG00000158258	64084	*CLSTN2*	0.9074
	ENSG00000110436	6506	*SLC1A2*	0.9073
	ENSG00000064393	28996	*HIPK2*	0.9073
	ENSG00000118482	23469	*PHF3*	0.907
	ENSG00000143970	55252	*ASXL2*	0.907
	ENSG00000135968	9648	*GCC2*	0.9

COMIR, combinatorial miRNA target prediction.

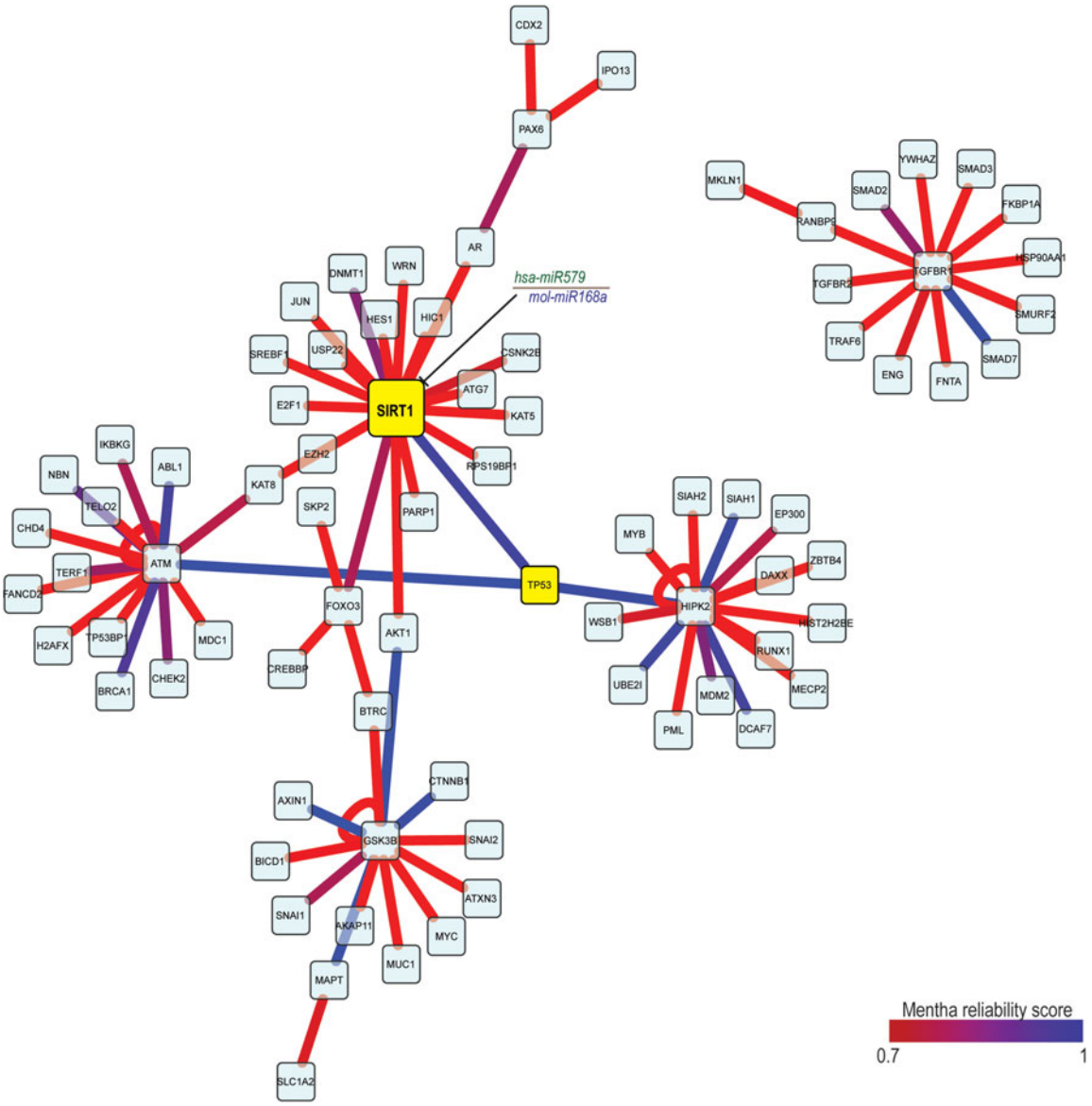

FIG. 4. Protein interaction analysis for the genes showing best COMIR score.

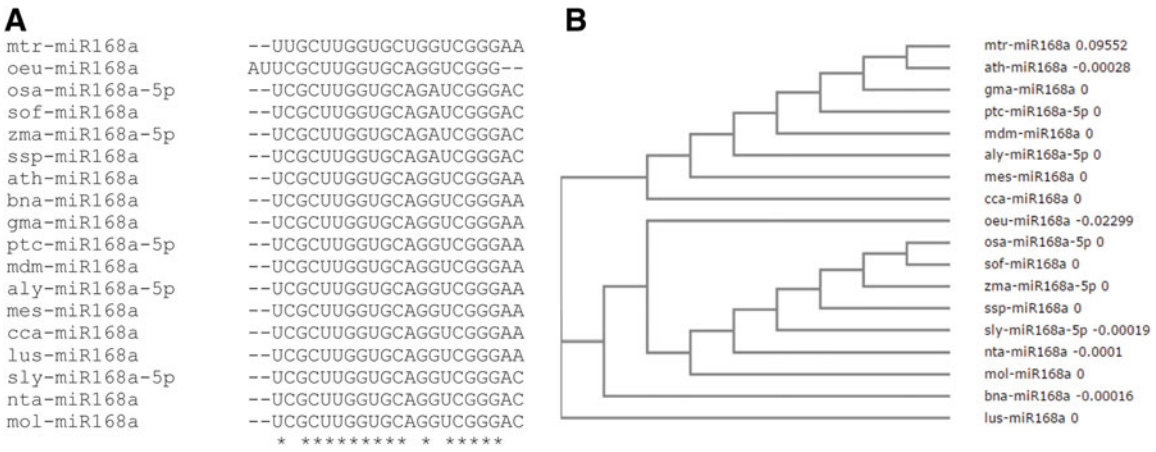

C

Family name	Sequence	Num. Members
ath-miR168a	UCGCUUGGUGCAGGUCGGGAA	9
osa-miR168a	UCGCUUGGUGCAGAUCGGGAC	4
mol-miR168a	UCGCUUGGUGCAGGUCGGGAC	3
oeu-miR168a	AUUCGCUUGGUGCAGGUCGGG	1

FIG. 5. Analysis of sequence conservation for *miR168a.* **(A)** Sequence alignment details with Clustal 2.1. **(B)** Dendrogram based on Euclidean distance between sequences. **(C)** Information summary for identified *miR168a* clusters.

from plant miRNA sequences in HEPG2 cell determined a significant decrease of *SIRT1* protein level in comparison with HF control samples (Fig. 7B, C).

4. DISCUSSION

The possibility to identify vegetal miRNAs able to bind and regulate the human genome expression will be of paramount importance for better knowledge of nutritional value of our foods.

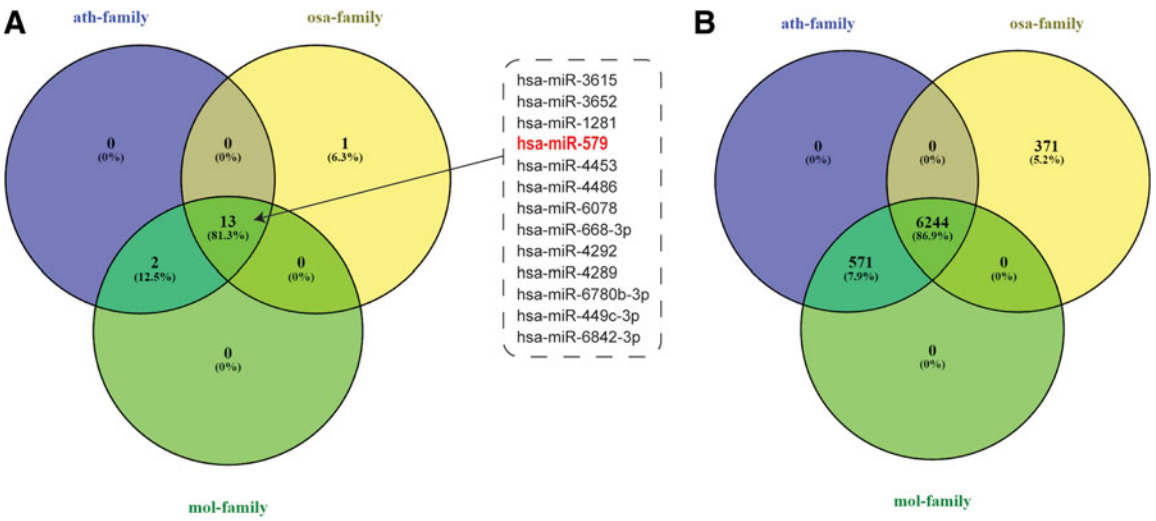

FIG. 6. Overlapping rate of putative human functional homologs **(A)** and target genes **(B)**, in *Arabidopsis thaliana (ath), Oryza sativa (osa)*, and *M. oleifera (mol) miR168a* groups.

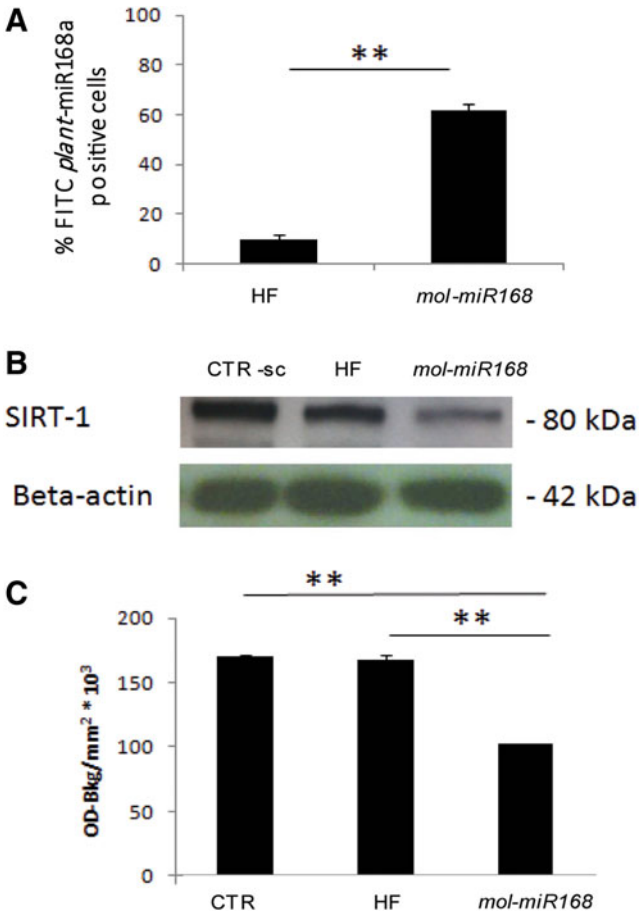

FIG. 7. . Experimental validation of miRNA-mRNA human gene regulation. **(A)** Percentage of positive cells 72 hours post-transfection with FITC-*mol-miR168a* in HEPG2 cells analyzed by flow cytometry. **(B)** One representative western blot assay of SIRT1 modulation after synthetic *mol-miR168a* transfection; *β-actin* expression, run on the same gel, indicates that an equal amount of protein was loaded for each sample. **(C)** Western blot analysis of SIRT1 expression was quantified by densitometry analysis, and values were expressed as OD-Bkg/mm$^2 \times 10^3$. Histograms represent mean value ± SD from three independent experiments performed on HEPG2 cells. Statistical comparison of means using *t*-test provided the following results: control 72 hours versus HF, not significant (NS); synthetic *mol-miR168a* versus control and versus HF, $^{**}p < 0.001$. FITC, fluorescein isothiocyanate. (Pirrò et al., 2016.)

From the studies of Zhang's group that first demonstrated the presence of *O. sativa* miRNAs in the sera and tissues of mice, the scientific community has much debated to better elucidate this discovery. In this context, functional miRNA studies demonstrated that ICR mice fed with plant total RNA in quantities of 10–50 μg showed *miR172* from *Brassica oleracea* as the most abundant exogenous miRNA in the sera, feces, and tissues in intestine, stomach, spleen, liver, and kidney (Liang et al., 2014). Encouraged by these discoveries, we shaped the concept of cross-kingdom functional homology, developing a completely new algorithm for the comparison of vegetal and mammalian miRNAs and implementing MirCompare, a free, fast, and user-friendly web application.

Given a collection of vegetal and plant miRNAs, MirCompare applies a double-layer filtering approach, respectively, based on overall and seed region homology rates.

Computational analysis on two different collections of stochastic sequences (10^2 and 10^3, respectively) showed that an *r*-value cutoff of 0.48 is required in the first-layer filtering, to extract statistically significant comparisons. This means that only 48% of overall homology between plant and mammalian miRNAs can lead to a functional correlation, emphasizing the concept of ''functional homology.'' According to the functional studies conducted by Brennecke et al., MirCompare further improves the analysis quality, applying a second-layer filter that takes into account only the comparisons, with strict homology related to seed region.

As study cases, *M. oleifera* and *H. sapiens* miRNomes have been provided to MirCompare to select a strict number of plant miRNA members with a potential genomic regulative role into human cells.

M. oleifera is one of the best known, most widely distributed, and most useful nutritional and medicinal plants (Anwar et al., 2006; Shahzad et al., 2013; Abdull Razis et al., 2014). The leaves are a source of natural antioxidants (Asma et al., 2005), vitamins, minerals, proteins, and essential amino acids (Anwar et al., 2006; Abdull Razis et al., 2014). A recent collaboration between universities in Italy and Cameroon has investigated the antioxidant and antitumor properties of *M. oleifera* (Canini, 2013).

Using low cutoff values for both the filtering layers, MirCompare highlighted 8 putative plant miRNAs with cross-kingdom potential, starting from 285,880 possible comparisons. Bioinformatic predictions of all the possible targets into human cell system for *M. oleifera* miRNAs highlighted a putative role of *mol-miR168a* in the active regulation of SIRT1. Protein network analysis highlighted the central role of SIRT1 in the regulation of P53 as a transcription factor. As well described by Gonfloni and collaborators, both SIRT1 and P53 regulate metabolism, stress signaling, cell survival, cell cycle control, and genome stability (Gonfloni et al., 2014).

Sequence analysis of *miR168a* sequences in 18 different plants show the presence of three different subfamilies that differ in one to two nucleotides. The synergic use of MirCompare and COMIR clarifies that small variations in *miR168a* sequences do not significantly affect homologies with human miRNAs (13) and their putative targets in humans (6244). Transfection experiments conducted by Pirrò et al. (2016) provided the formal evidence that *mol-miR168a* identified by MirCompare inhibits the translation of SIRT1, when their synthetic mimics are transfected into the cancer cell line HEPG2.

Further analysis will be carried out to better investigate the molecular mechanisms underlying the cross-kingdom interactions highlighted by MirCompare. Additional molecular and pharmaceutical approaches need to validate the clinical utilization of plant miRNAs in the treatment of cancer and other dysregulatory diseases. The ease of use of our web application, coupled with its high calculation speed, and flexibility in the selection of analysis parameters may help and allow the scientific community to better focus their attention on the cross-kingdom regulation mediated by plants and all the possible implications in the treatment of several diseases. This article mainly focuses the attention on the concept that cross-kingdom regulation of human genome is not a peculiar funding, as suggested by Zhang et al. in 2012, but a more generalized phenomenon linked to the historical Greek medical concept that ''we are what we eat.''

ACKNOWLEDGMENTS

The authors thank Dr. Alberto Calderone, Institute for Systems Analysis and Computer Science ''Antonio Ruberti''—National Research Council, Professor Massimo Amicosante, Department of Biomedicine and Prevention, University of Rome ''Tor Vergata,'' Dr. Marco Cirilli and Professor Rosario Muleo, Department of Science and Technology for Agriculture, Forestry, Nature, and Energy, University ''La Tuscia,'' Viterbo for language revision and helpful discussion.

AUTHOR DISCLOSURE STATEMENT

No competing financial interests exist.

REFERENCES

Abdull Razis, A.F., Ibrahim, M.D., and Kntayya, S.B. 2014. Health benefits of *Moringa oleifera*. *Asian Pac. J. Cancer Prev.* 15, 8571–8576.

Anwar, F., Latif, S., Ashraf, M., et al. 2006. *Moringa oleifera*: a food plant with multiple medicinal uses. *Phytother. Res.* 21, 17–25.

Asma, S., Farooq, A., Maleeha, M., et al. 2005. Antioxidant activity of different solvent extracts of *Moringa oleifera* leaves under accelerated storage of sunflower oil. *Asian J. Plant Sci.* 4, 630–635.

Baldrich, P., and San Segundo, B. 2016. MicroRNAs in rice innate immunity. *Rice (N.Y.).* 9, 6.

Bartel, D.P. 2009. MicroRNAs: Target recognition and regulatory functions. *Cell.* 136, 215–233.

Bradbury, C.A., Khanim, F.L., Hayden, R., et al. 2005. Histone deacetylases in acute myeloid leukaemia show a distinctive pattern of expression that changes selectively in response to deacetylase inhibitors. *Leukemia.* 19, 1751–1759.

Brennecke, J., Stark, A., Russell, R.B., et al. 2005. Principles of microRNA–target recognition. *PLoS Biol.* 3, e85.

Buck, A.H., Coakley, G., Simbari, F., et al. 2014. Exosomes secreted by nematode parasites transfer small RNAs to mammalian cells and modulate innate immunity. *Nat. Commun.* 5, 5488.

Calderone, A., Castagnoli, L., and Cesareni, G. 2013. mentha: a resource for browsing integrated protein-interaction networks. *Nat. Methods.* 10, 690–691.

Canini, A. 2013. Antioxidant extracts of African medicinal plants induce cell cycle arrest and differentiation in B16F10 melanoma cells. *Int. J. Oncol.* 43, 956–964. Available at: http://dx.doi.org/10.3892/ijo.2013.2001

Chin, A.R., Fong, M.Y., Somlo, G., et al. 2016. Cross-kingdom inhibition of breast cancer growth by plant miR159. *Cell Res.* 26, 217–228.

Coronnello, C., and Benos, P.V. 2013. ComiR: combinatorial microRNA target prediction tool. *Nucleic Acids Res.* 41, W159–W164.

Cui, Y., Han, J., Xiao, Z., et al. 2016. The miR-20-Rest-Wnt signaling axis regulates neural progenitor cell differentiation. *Sci. Rep.* 6, 23300.

Del Fabbro, C., Scalabrin, S., Morgante, M., et al. 2013. An extensive evaluation of read trimming effects on Illumina NGS data analysis. *PLoS One.* 8, e85024.

Dickinson, B., Zhang, Y., Petrick, J.S., et al. 2013. Lack of detectable oral bioavailability of plant microRNAs after feeding in mice. *Nat Biotechnol.* 31, 965–967.

Dileepan, M., Sarver, A.E., Rao, S.P., et al. 2016. MicroRNA mediated chemokine responses in human airway smooth muscle cells. *PLoS One.* 11, e0150842.

El Gazzar, M., and McCall, C.E. 2010. MicroRNAs distinguish translational from transcriptional silencing during endotoxin tolerance. *J. Biol. Chem.* 285, 20940–20951.

Feng, J., and Chen, J. 2013. In silico analysis the complementarity of tomato microRNA/microRNA* sequences with cucumber mosaic virus (CMV) genomic RNAs. *J. Nanosci. Nanotechnol.* 13, 4421–4426.

Frixa, T., Donzelli, S., and Blandino, G. 2015. Oncogenic microRNAs: key players in malignant transformation. *Cancers.* 7, 2466–2485.

Gonfloni, S., Iannizzotto, V., Maiani, E., et al. 2014. P53 and Sirt1: routes of metabolism and genome stability. *Biochem. Pharmacol.* 92, 149–156.

Gurtner, A., Falcone, E., Garibaldi, F., et al. 2016. Dysregulation of microRNA biogenesis in cancer: the impact of mutant p53 on Drosha complex activity. *J. Exp. Clin. Cancer Res.* 35, 45.

Han, L., and Luan, Y.-S. 2015. Horizontal transfer of small RNAs to and from plants. *Frontiers in Plant Science* [online], 6. Available at: www.ncbi.nlm.nih.gov/pmc/articles/PMC4674566. Accessed March 22, 2016.

Huang, Y., Shen, X.J., Zou, Q., et al. 2010. Biological functions of microRNAs. *Russian J. Bioorg. Chem.* 36, 684–689.

Huffman, D.M., Grizzle, W.E., Bamman, M.M., et al. 2007. SIRT1 is significantly elevated in mouse and human prostate cancer. *Cancer Res.* 67, 6612–6618.

Inoue, Y., Iemura, S., Natsume, T., et al. 2011. Suppression of p53 activity through the cooperative action of Ski and histone deacetylase SIRT1. *J. Biol. Chem.* 286, 6311–6320.

Jain, A.K., Allton, K., Iacovino, M., et al. 2012. p53 regulates cell cycle and microRNAs to promote differentiation of human embryonic stem cells. *PLoS Biol.* 10, e1001268.

John, B., Enright, A.J., Aravin, A., et al. 2004. Human microRNA targets. *PLoS Biol.* 2, e363.

Jones-Rhoades, M.W. 2011. Conservation and divergence in plant microRNAs. *Plant Mol. Biol.* 80, 3–16.

Kertesz, M., Iovino, N., Unnerstall, U., et al. 2007. The role of site accessibility in microRNA target recognition. *Nat. Genet.* 39, 1278–1284.

Kim, E.-J., Kho, J.-H., Kang, M.-R., et al. 2007. Active regulator of SIRT1 cooperates with SIRT1 and facilitates suppression of p53 activity. *Mol. Cell.* 28, 277–290.

Kim, J.-E., Chen, J., and Lou, Z. 2008. DBC1 is a negative regulator of SIRT1. *Nature.* 451, 583–586.

Kozomara, A., and Griffiths-Jones, S. 2010. miRBase: integrating microRNA annotation and deep-sequencing data. *Nucleic Acids Res.* 39, D152–D157.

Krek, A., Grün, D., Poy, M.N., et al. 2005. Combinatorial microRNA target predictions. *Nat. Genet.* 37, 495–500.

LaMonte, G., Philip, N., Reardon, J., et al. 2012. Translocation of sickle cell erythrocyte microRNAs into *Plasmodium falciparum* inhibits parasite translation and contributes to malaria resistance. *Cell Host Microbe.* 12, 187–199.

Langley, E., Pearson, M., Faretta, M., et al. 2002. Human SIR2 deacetylates p53 and antagonizes PML/p53-induced cellular senescence. *EMBO J.* 21, 2383–2396.

Larkin, M.A., Blackshields, G., Brown, N.P., et al. 2007. Clustal W and clustal X version 2.0. *Bioinformatics.* 23, 2947–2948.

Lee, H.-M., Kim, T.S., and Jo, E.-K. 2016. MiR-146 and miR-125 in regulation of innate immunity and inflammation. *BMB Rep.* [Epub ahead of print] P11: 3526.

Lewis, B.P., Burge, C.B., and Bartel, D.P. 2005. Conserved seed pairing, often flanked by adenosines, indicates that thousands of human genes are microRNA targets. *Cell.* 120, 15–20.

Liang, G., Zhu, Y., Sun, B., et al. 2014. Assessing the survival of exogenous plant microRNA in mice. *Food Sci. Nutr.* 2, 380–388.

Li, J., Feng, Z., Chen, L., et al. 2016. MicroRNA-335-5p inhibits osteoblast apoptosis induced by high glucose. *Mol. Med. Rep.* 13, 4108–4112.

Liu, Q., Wang, F., and Axtell, M.J. 2014. Analysis of complementarity requirements for plant microRNA targeting using a *Nicotiana benthamiana* quantitative transient assay. *Plant Cell.* 26, 741–753.

Liu, X., Wang, D., Zhao, Y., et al. 2011. Methyltransferase Set7/9 regulates p53 activity by interacting with sirtuin 1 (SIRT1). *Proc. Natl. Acad. Sci. U. S. A.* 108, 1925–1930.

Li, Y., and Sarkar, F.H. 2016. MicroRNA Targeted therapeutic approach for pancreatic cancer. *Int. J. Biol. Sci.* 12, 326–337.

Lukasik, A., and Zielenkiewicz, P. 2014. In silico identification of plant miRNAs in mammalian breast milk exosomes–a small step forward? *PLoS One* [online], 9. Available at: www.ncbi.nlm.nih.gov/pmc/articles/PMC4059707/. Accessed March 22, 2016.

Ma, Z.-X., Tan, X., Shen, Y., et al. 2015. MicroRNA expression profile of mature dendritic cell in chronic rhinosinusitis. *Inflamm. Res.* 64, 885–893.

Mallory, A.C., Reinhart, B.J., Jones-Rhoades, M.W., et al. 2004. MicroRNA control of PHABULOSA in leaf development: importance of pairing to the microRNA 5′ region. *EMBO J.* 23, 3356–3364.

Pirrò, S., Zanella, L., Kenzo, M., et al. 2016. MicroRNA from *Moringa oleifera*: identification by high throughput sequencing and their potential contribution to plant medicinal value. *PLoS One.* 11, e0149495.

Sadovsky, Y., Mouillet, J.-F., Ouyang, Y., et al. 2015. The function of TrophomiRs and other microRNAs in the human placenta. *Cold Spring Harb. Perspect. Med.* 5, a023036.

Sala-Cirtog, M., Marian, C., and Anghel, A. 2015. New insights of medicinal plant therapeutic activity—the miRNA transfer. *Biomed. Pharmacother.* 74, 228–232.

Shahzad, U., Khan, M.A., Jaskani, M.J., et al. 2013. Genetic diversity and population structure of *Moringa oleifera*. *Conserv. Genet.* 14, 1161–1172.

Shannon, P., Markiel, A., Ozier, O., et al. 2003. Cytoscape: a software environment for integrated models of biomolecular interaction networks. *Genome Res.* 13, 2498–2504.

Shu, J., Chiang, K., Zempleni, J., et al. 2015. Computational characterization of exogenous microRNAs that can be transferred into human circulation. *PLoS One.* 10, e0140587.

Snow, J.W., Hale, A.E., Isaacs, S.K., et al. 2013. Ineffective delivery of diet-derived microRNAs to recipient animal organisms. *RNA Biol.* 10, 1107–1116.

Stünkel, W., Peh, B.K., Tan, Y.C., et al. 2007. Function of the SIRT1 protein deacetylase in cancer. *Biotechnol. J.* 2, 1360–1368.

Wang, B. 2013. Base composition characteristics of mammalian miRNAs. *J. Nucleic Acids.* 2013, 1–6.

Xie, M., Zhang, S., and Yu, B. 2015. microRNA biogenesis, degradation and activity in plants. *Cell. Mol. Life Sci.* 72, 87–99.

Xie, X., Song, J., and Li, G. 2016. MiR-21a-5p suppresses bisphenol A-induced pre-adipocyte differentiation by targeting map2k3 through MKK3/p38/MAPK. *Biochem. Biophys. Res. Commun.* 473, 140–146.

Xing, T., Xu, H., Yu, W., et al. 2015. Expression profile and clinical significance of miRNAs at different stages of chronic hepatitis B virus infection. *Int. J. Clin. Exp. Med.* 8, 5611.

Zhang, L., Hou, D., Chen, X., et al. 2011. Exogenous plant MIR168a specifically targets mammalian LDLRAP1: evidence of cross-kingdom regulation by microRNA. *Cell Res.* 22, 107–126.

Zhao, W., Kruse, J.-P., Tang, Y., et al. 2008. Negative regulation of the deacetylase SIRT1 by DBC1. *Nature.* 451, 587–590.

Address correspondence to:
Stefano Pirrò, PhD Student
Department of Biology
University of Rome ''Tor Vergata''
Via della Ricerca Scientifica
Rome 00133
Italy

E-mail: stefano.pirro@uniroma2.it